N95- 28838

Impact Damage Resistance of Composite Fuselage Structure, Part 2[1]

by

Ernest F. Dost, Scott R. Finn,

Daniel P. Murphy, and Amy B. Huisken

The Boeing Company, Seattle, WA

Introduction

The strength of laminated composite materials may be significantly reduced by foreign object impact induced damage. An understanding of the damage state is required in order to predict the behavior of structure under operational loads or to optimize the structural configuration. Types of damage typically induced in laminated materials during an impact event include transverse matrix cracking, delamination, and/or fiber breakage. The details of the damage state and its influence on structural behavior depend on the location of the impact. Damage in the skin may act as a soft inclusion [1] or affect panel stability [2], while damage occurring over a stiffener may include debonding of the stiffener flange from the skin.
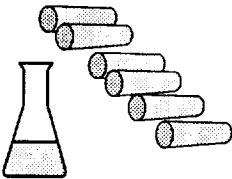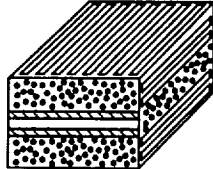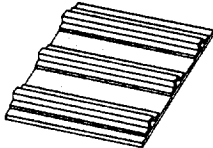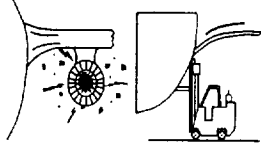
An experiment to characterize impact damage resistance of fuselage structure as a function of structural configuration and impact threat was performed [3]. A wide range of variables associated with aircraft fuselage structure such as material type and stiffener geometry (termed, intrinsic variables) and variables related to the operating environment such as impactor mass and diameter (termed, extrinsic variables) were studied using a statistically based design-of-experiments technique. The experimental design resulted in thirty-two different 3-stiffener panels. These configured panels were impacted in various locations with a number of impactor configurations, weights, and energies. The results obtained from an examination of impacts in the skin midbay and hail simulation impacts were documented in [3]. The current discussion is a continuation of that work with a focus on non-discrete characterization of the midbay hail simulation impacts and discrete characterization of impact damage for impacts over the stiffener.

Nine variables associated with aircraft fuselage structure and six variables associated with potential foreign object impact threats were investigated to determine the relative importance of each variable to different composite failure modes. The intrinsic variable levels (e.g., 938 epoxy versus 977-2 toughened epoxy for the variable: Matrix type) were chosen based on performance and assembly requirements for a widebody transport aircraft fuselage. The extrinsic variable levels (e.g., flat versus spherical for the variable: Impactor shape) were selected to represent a wide range of potential threats from runway debris to dropped tools.

The experiment was designed as a fractional factorial, resolution IV designed experiment [4] in order to study this large number of variables with a relatively small number of specimens. Fourteen variables were included directly in a designed experiment which defined 32 three-stiffener panels. The fifteenth variable was built into each panel by placing a layer adhesive between the skin and two of the three stiffeners during panel assembly. One-hundred and ten inch long panels were fabricated which included both thick and thin sections of equal length, separated by a 10 inch tapered region. This introduced a split-plot aspect to the experiment [5], creating two sizes of experimental units. The intrinsic variables, except laminate thickness, are "whole-plot" variables, while the extrinsic variables along with laminate thickness are "sub-plot" variables. The highly fractionated nature of this experiment created some confounding of effects. Main effects are confounded with three-factor and higher order interaction effects, and two-factor interaction effects are confounded with other two-factor effects.

Intrinsic and Extrinsic Variables Studied

Intrinsic Variables			Extrinsic Variables
Material Variables	Laminate Variables	Structural Variables	

Fiber
● AS4
● IM7

Resin
● 938 (3501-6)
● 977-2

Fiber volume
● 0.480
● 0.565

Material form
● Tape
● Tow

Stiffener layup
● Hard
● Soft

Skin layup
● Hard
● Soft

Thickness
● Thick
  ● Skin 0.18 in
  ● Stiffener 0.12 in
● Thin
  ● Skin 0.09 in
  ● Stiffener 0.06 in

Stiffener type
● Blade
● Hat

Stiffener spacing
● 7 in
● 12 in

Stiffener adhesive layer
● With
● Without

Impactor mass
● 0.62 lbm
● 13.9 lbm

Impact energy (skin/stiffener)
● 200 in-lb/350 in-lb
● 1,200 in-lb/1,600 in-lb

Impact temperature
● 70°F
● 180°F

Impactor diameter
● 0.25 in
● 1.0 in

Impactor tup shape
● Flat
● Spherical

Impactor stiffness
● 0.4 Msi
● 30 Msi

The panel configurations and materials chosen for the impact damage resistance designed experiment are representative of a variety of locations around the fuselage. The fuselage crown is a tension dominated structure and hence a wide stiffener spacing and thin skin gages can be used. The fuselage lower side-panel on the other hand is combined compression/shear dominated and requires a close stiffener spacing and thicker gages. A matrix with high interlaminar toughness may be required for the lower side-panel when considering the high levels of impact energy resulting from runway debris impacts. The crown, however, has hail impact as a design criteria and may not require costly toughened materials to resist damage from these events. The panels built for this experiment have combinations of the variables covering a range of locations on the fuselage.

Fuselage Locations Represented by Test Panels
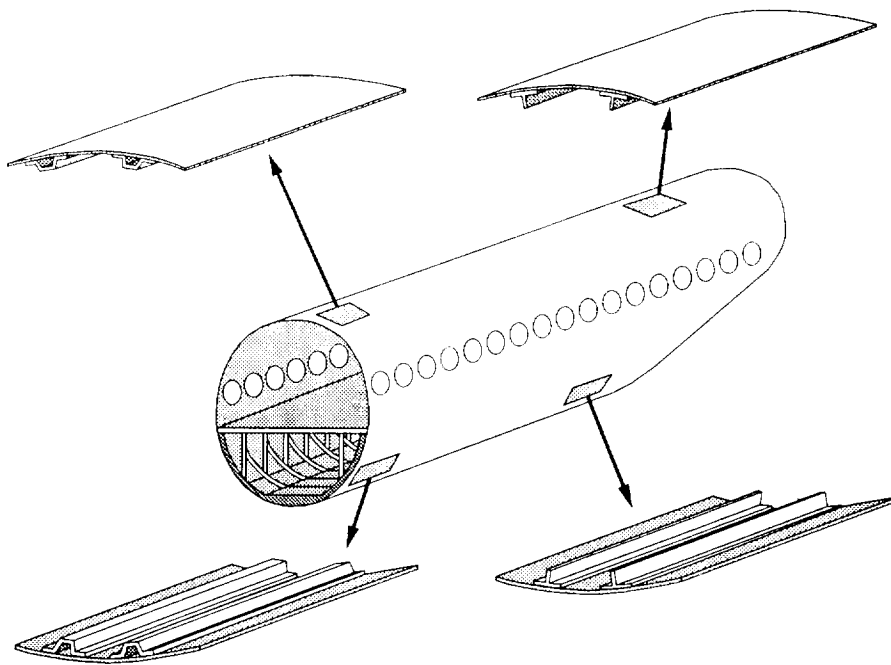
| NASA/BOEING | ED-03 |
| ATCAS | FL2014.03 s |

The damage states associated with the impact locations shown below were studied on all 32 impact damage resistance panels. These locations were believed to represent those most critical for stiffened structure of this sort. Various responses (e.g., C-scan area) were measured at each impact site. Statistical analyses of the results for each impact location were analyzed as if each location were a separate parallel experiment.

Impact Locations Studied
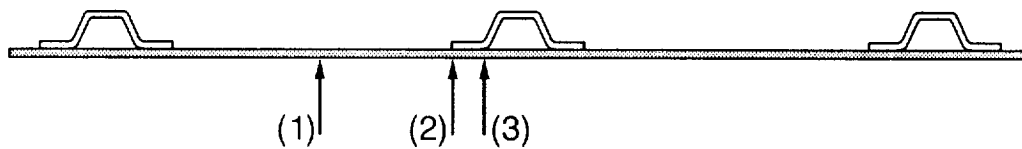
(1) Hail simulation
(2) Edge of stiffener attachment flange
(3) Base of stiffener web

| NASA/BOEING | ED-04 |
| ATCAS | FL2014.04 s1h |

762
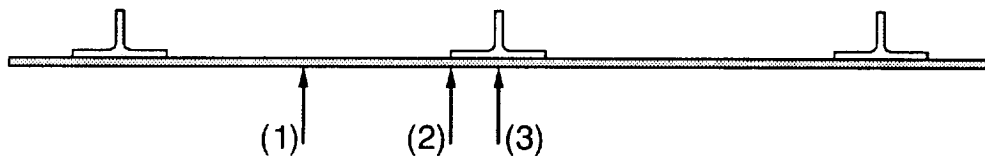
The purpose of this experiment was to determine the response of configured fuselage structure to foreign object impact. The responses measured for the impact locations discussed previously included: a) maximum force during the impact event for the stiffener web and flange edge impacts, b) local flexural stiffness of the midbay hail simulation impacts, c) matrix damage associated with load redistribution failures, and d) matrix damage which could act as an initial flaw for stiffener separation under operational loads.

Measured Responses

- Maximum force

- Local flexural stiffness

- Localized core-damage area

- Stiffener flange separation
  - Area (stiffener cocured with adhesive)
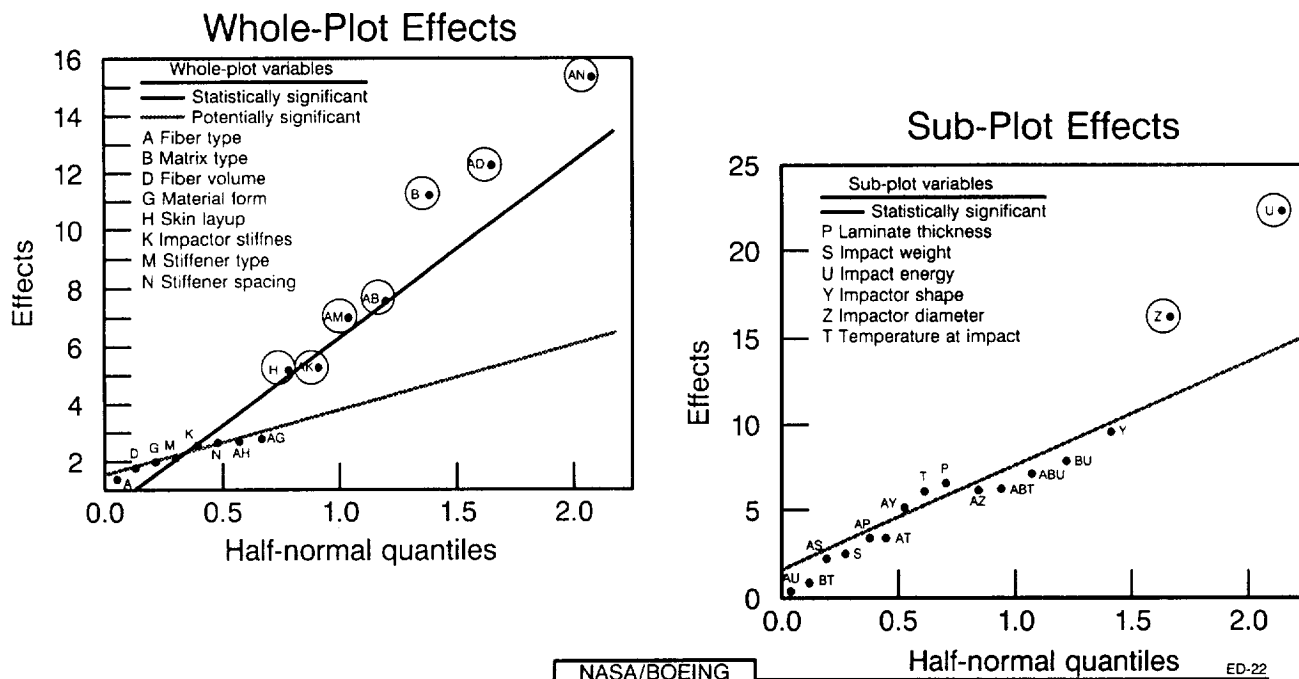 - Area (stiffener cocured without adhesive)
  - Ratio (with adhesive/without adhesive)

The highly fractionated and non-replicated nature of this experimental design made it impossible to use a straightforward Analysis of Variance (ANOVA) model to analyze the data. In such situations, there are two different techniques which may be employed. The first is to use a reduced ANOVA model, in which some of the higher-order interactions are *a priori* assumed to be insignificant. The corresponding sums of squares are pooled to form a residual sum of squares which is used as an estimate of the experimental error. The second option is to construct half-normal plots [6] of the effect estimates. The split-plot [5] aspect of this experimental design made the pooling of higher-order interaction terms very arbitrary. For this reason, the second option was chosen to analyze the results.

The half-normal plot is a plot of the absolute values of the ordered effect estimates against $\phi^{-1}(i/(n+1))$, where i is the rank of the particular effect estimate, n is the number of effect estimates to be plotted, and ϕ^{-1} is the inverse of the standard normal probability distribution. This is based on the ANOVA assumption that the effect estimates will constitute a random sample from some normal distribution if no significant effects exist. A lack of significant effects will result in the half-normal probability plot being approximately linear. A large deviation from the linear pattern indicates a significant effect. The split-plot aspect of this experimental design was accounted for by constructing two half-normal plots, one corresponding to the whole-plot effects and the other to the half-plot effects.

Statistical Data Analysis

Half-Normal Plots

Whole-Plot Effects

Whole-plot variables
—— Statistically significant
----- Potentially significant
A Fiber type
B Matrix type
D Fiber volume
G Material form
H Skin layup
K Impactor stiffnes
M Stiffener type
N Stiffener spacing

Effects axis: 16, 14, 12, 10, 8, 6, 4, 2

Half-normal quantiles: 0.0 0.5 1.0 1.5 2.0

Sub-Plot Effects

Sub-plot variables
—— Statistically significant
P Laminate thickness
S Impact weight
U Impact energy
Y Impactor shape
Z Impactor diameter
T Temperature at impact

Effects axis: 25, 20, 15, 10, 5, 0

Half-normal quantiles: 0.0 0.5 1.0 1.5 2.0

ED-22

FL2014.22 h1h

Response Measurement Definition

The majority of impacts were performed with an instrumented impactor (i.e., impactor contains a load cell). The load cell recorded impact force as a function of time, while initial impactor velocities were measured using a set of light gates. These data were numerically integrated to calculate velocity, displacement, and energy as a function of time [7]. Plotted below are force versus time results for both a high mass and a low mass impact on two different panels for a fixed impact energy level. A large number of different metrics can be defined to characterize these impact events, including the maximum force, force at first load drop, duration of the event, and frequencies of the oscillations. Additionally, calculated values such as maximum deflection or absorbed energy can be used to characterize the impact event. Recent work has suggested that maximum force may be a better measure than impact energy for comparing impact damage resistance on different sized parts. Therefore, for this study we selected maximum force as our response variable.

Maximum Force (During Impact Event)

Response Measurement Definition

Low Mass -
High-Energy Impact

High Mass -
High-Energy Impact
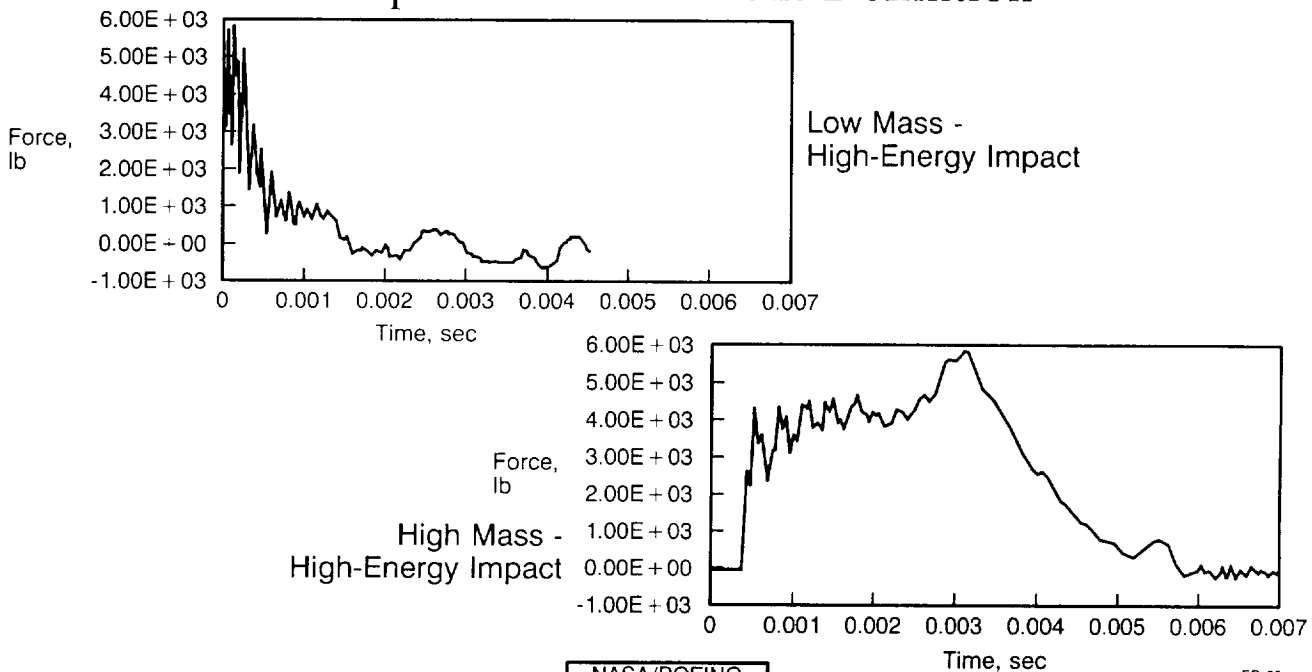
NASA/BOEING
ATCAS

ED-20

FL2014.20 s1h

765

Finite element modeling of several of the impact events was performed to gain understanding into interactions of the stiffeners and skin, and the interactions of the impactor and panel. Such analyses, if sufficiently accurate, would provide valuable information pertaining to strain levels throughout the test specimen and would allow for extrapolation of test panel data to predict aircraft structure response. These analyses are technically very challenging in that they require the prediction of the dynamic response of an extremely nonlinear system. The large lateral deflections and coupling between the skin, stiffeners, and the clamped pine support blocks are complex.

Analytical simulations of six test events in which no detectable damage was found were conducted using the explicit, nonlinear structural dynamics finite element analysis code DYNA3D [8]. The critical distinction of an explicit code from the standard implicit code (e.g., NASTRAN, STAGSC-1) is that in solving a transient problem, the solution can be advanced in time without solving large systems of equations, (i.e., the equations of motion of a structural system are uniquely uncoupled). This permits the local incorporation of nonlinear phenomena such as plasticity, impact, penetration, and large deflections without having to periodically reformulate the entire problem.

The panels were modeled with shell elements and a linearly elastic orthotropic material description. Modeling the pine support blocks with solid elements was found to be a key factor in obtaining accurate results. Solid elements with linear elastic pine properties realistically reproduced the local out of plane rotation of the panel at its boundaries, which was shown to contribute as much as 40% of the lateral deflection as measured by the instrumented impactor. The impactor was modeled with solid elements for the tup, beam elements for the load cell, and lumped mass elements for the mass behind the load cell.

DYNA3D Model Geometry

Impactor (13.975 lb)

Pine support blocks

Panel
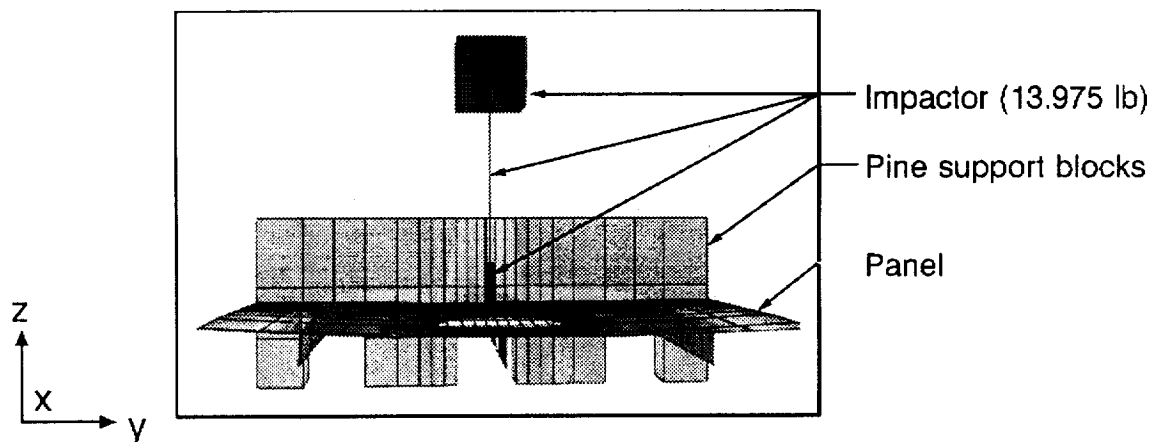
Model Statistics
- 983 node points
- 212 continuum (8-node brick) elements
- 576 Hughes-Liu shell elements
- 3 Hughes-Liu beam elements
- Run time: 62 CPU sec - CRAY Y-MP

A large variety of computed values can be extracted from a DYNA3D simulation. Stresses, strains, forces, and the motion of the individual elements and node points can be plotted as a function of time. In addition, "snapshots" of the entire structure can be obtained at any time of interest within the period of simulation. The example shown here displays the deformed geometry of the model (wooden supports and impactor excluded for clarity) with the lower surface strains plotted on the structure. The magnitude of strain is indicated by the shades of gray distributed across the figure. These snapshots allow rapid identification of "hot spots" (i.e., areas of high strain) and areas of interest, while the time histories allow quick determination of the time and magnitude of maximum response. A series of snapshots can be combined, allowing for an animated display of the model response. By viewing its motion and a range of stress and strain components as their values vary with time, valuable insights to the response of the test event can be gained. The visual interaction of membrane and flexural modes is of particular interest, as is the time lag between the peak response in the panel and in the peak responses of the stiffeners.

## *DYNA3D Stiffener Impact Analysis*

Surface Strains

| NASA/BOEING	ED-06
ATCAS	FL2014HR.06 h1h

767
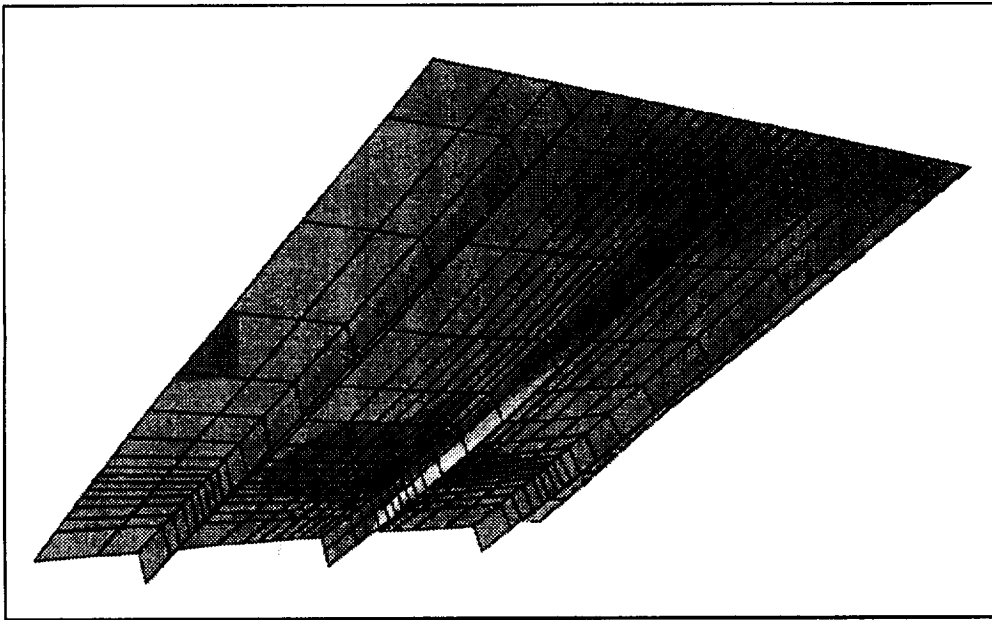
In the next two figures, the calculated responses are compared to test data for two impact events occurring over the centerline of blade stiffeners. Both of these tests were performed on "thick" panels with closely spaced stiffeners, resulting in a rather stiff target. Note that the time scale of the DYNA3D result is shifted to permit a distinction to be made from the test data. Note also that the impact energy for the second test is nearly five times that of the first, while the peak responses (force and displacement) are only doubled. In both tests the displacement response is very accurately predicted. In the force versus time comparisons, the duration of the low frequency response is very well predicted, as is the high frequency component of the response. Peak forces are, in general, accurately predicted for the first 2.5 milliseconds (msec) and the last 3 msec. However, at about 3 msec the analysis underpredicts the force levels. This has been observed in all of the studies made, and the source of the error is not completely understood. A local numerical instability of the finite elements representing the impactor tip (known as "hourglassing") is observed in this portion of the analysis, and may be responsible. However, further analyses should be conducted to investigate this effect further. Recovery of strain energy from indentation of the panel by the impactor might also be a source of additional force in the impactor's transducer. The shell elements used for all analyses to date cannot reproduce this phenomenon, but solid elements or nonlinear springs could easily be added to the impact region to explore this possibility.

Blade Stiffener Centerline Low-Energy Impact

Mass = 13.98 lb
Velocity = 11.6 ft/s
Energy = 349 in-lb

Flat 1/4-in Graphite Tip

768
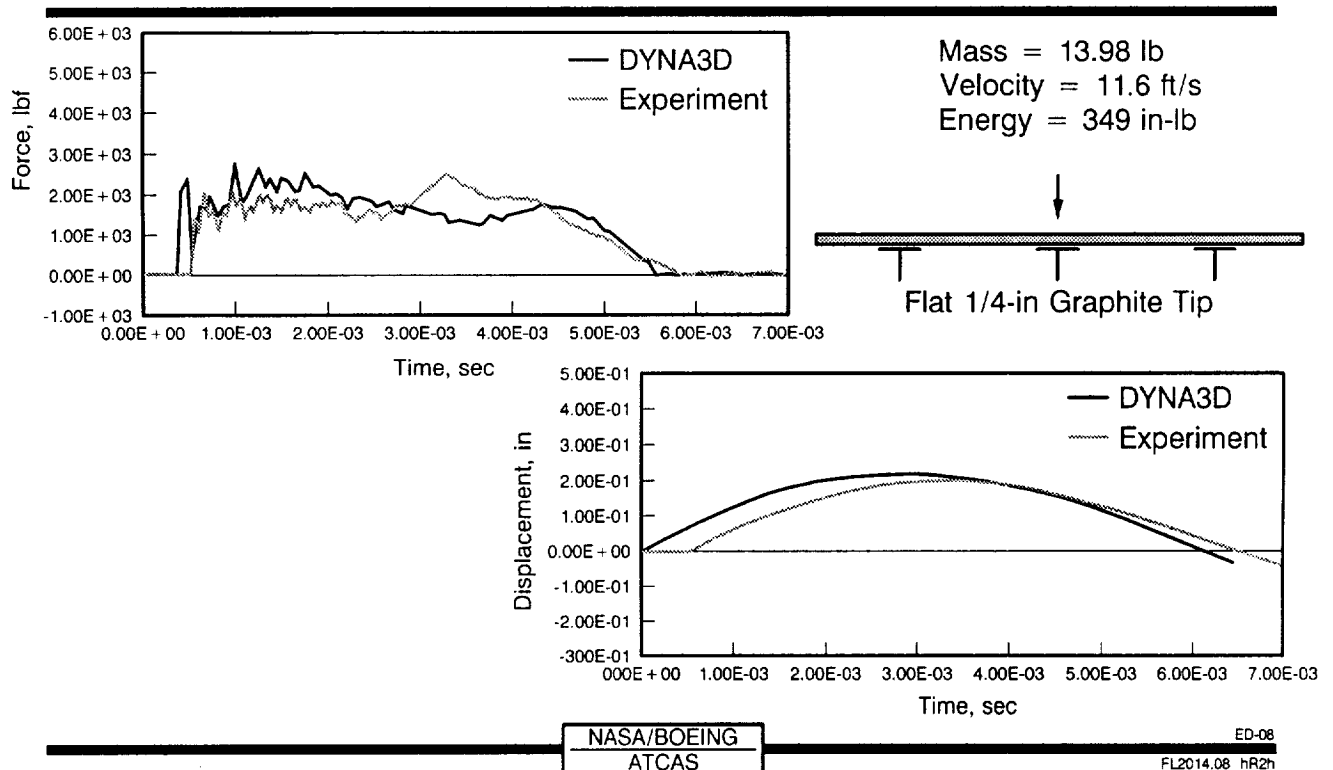
Blade Stiffener Centerline High-Energy Impact
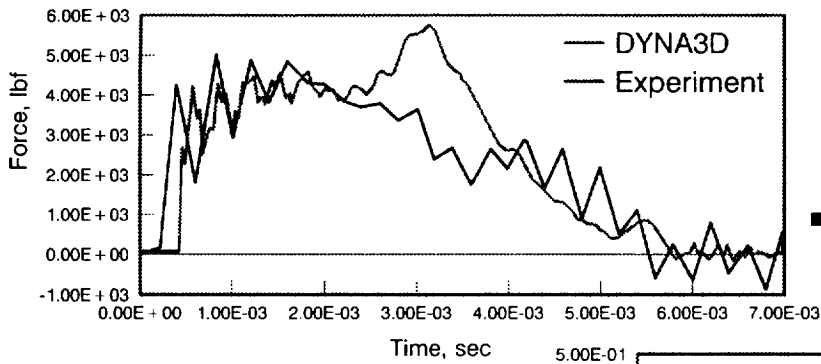
Mass = 13.98 lb
Velocity = 24.7 ft/s
Energy = 1,589 in-lb

Flat 1/4-in Graphite Tip
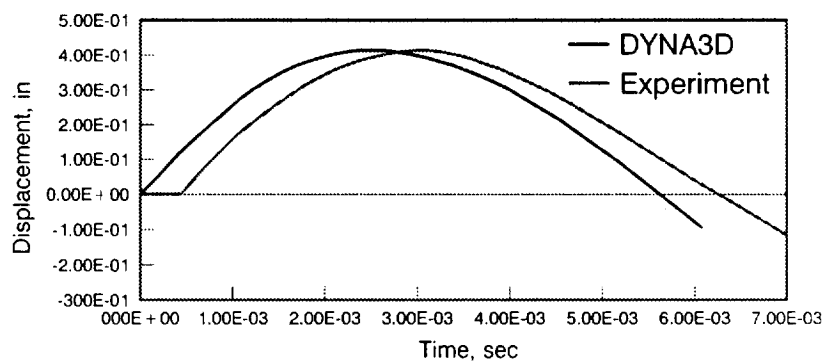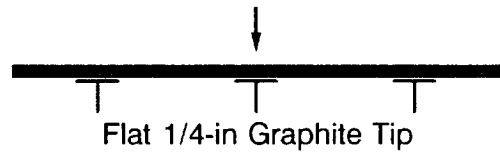
ED-09

F2014.09 hR2h

Significant Effects

The maximum forces for both the stiffener flange edge and stiffener web impacts were analyzed using half-normal plots as previously discussed. The statistical analysis showed the variables listed below to have significant effects on the maximum force developed during the impact event. The letter preceding each variable indicates the impact location for which the listed variable was found to be significant. A variable is significant for both sets of impacts if both letters are listed. In addition to the five main effects, 2 sets of two-way interactions are important. Each set of confounded two-way interactions also included four additional interactions which were not listed for brevity.

There are several observations to be made concerning these results. The first is that impact mass has a stronger effect on impact force than the impact energy. It should be noted that the higher energy impacts tended to perforate the panel, limiting the influence of this variable on maximum force. The variables associated with the impactor geometry (shape and diameter) have a strong influence on the peak forces. The two-way interactions that are listed were chosen because the individual variables also appear as main effects; therefore, the likelihood of these interactions being significant is greater than that of the other interactions with which they are confounded.

Maximum Force

Significant Effects

Impact location	Variable	Low level	High level	Result
F,W	Impact mass, lbm	0.62	13.97	Decreased
F,W	Laminate thickness, in	0.089	0.18	Increased
F,W	Impact energy, in-lb	350	1,600	Increased
F,W	Impactor diameter, in	0.25	1.00	Increased
F,W	Impactor shape	Flat	Spherical	Decreased

Important Interactions

W Laminate thickness - Impactor diameter or Impactor mass - Impactor shape or ?

F Impactor shape - Impactor diameter or Laminate thickness - Impact mass or ?

F (flange) W (web)

NASA/BOEING		ED-21
ATCAS		FL2014.21 hR2h

Response Measurement Definition

Impact damage in a composite laminate generally consists of some combination of matrix damage and fiber failures. The performance of a laminate with damage is related to the stability of sublaminates created by the matrix damage [1,9,10] and the extent of fiber failures [11]. The damage region behaves as a "soft zone" under load, with loads redistributing around buckled sublaminates and broken fibers. The local out-of-plane (flexural and transverse shear) stiffness of the damage zone should relate directly to the stiffness of the damage region under load. A quantitative measure of this flexural stiffness may allow the direct calculation of the influence of the damage on structural performance without detailed determination of the through-thickness location of all delaminations, transverse cracks, and fiber breaks.

Local Flexural Stiffness

Response Measurement Definition

Directly
related

Local Flexural Stiffness - Damaged Normalized by Undamaged

CAI Sublaminate
Buckling
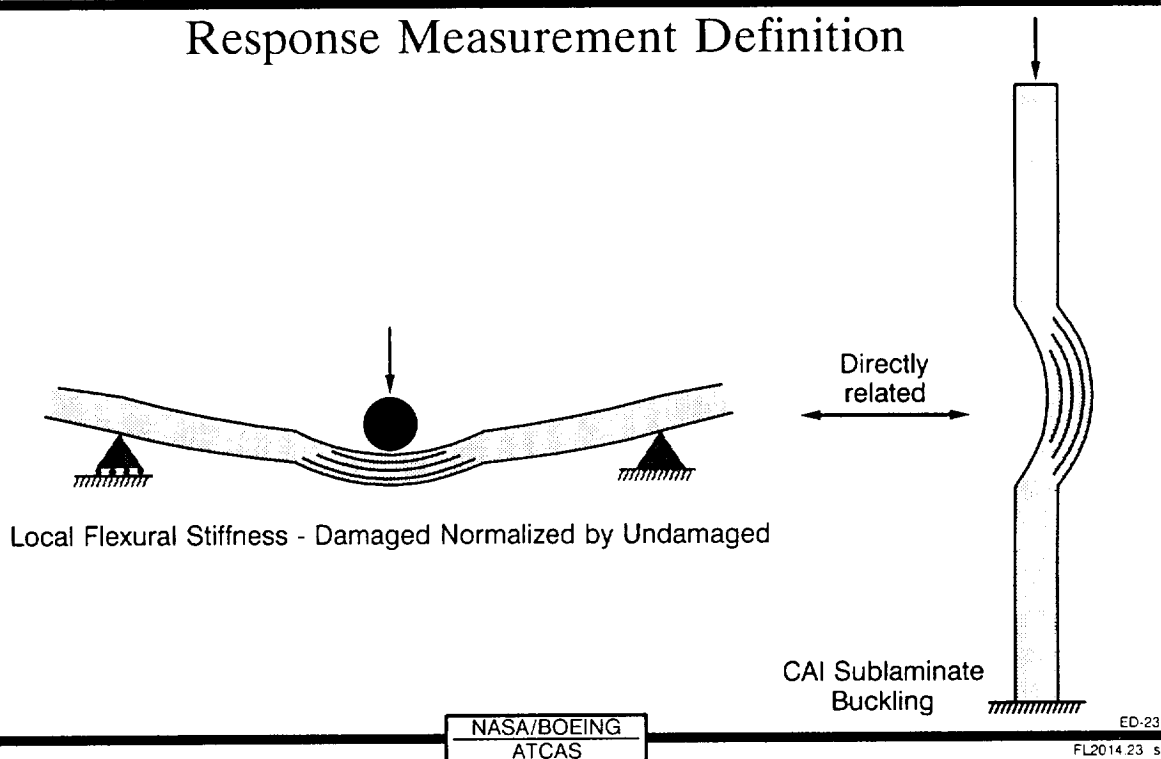
NASA/BOEING
ATCAS

ED-23
FL2014.23 s

771

An inspection method based on flexural wave propagation [10,12] was used to estimate stiffness reductions in panel mid-bay regions subjected to hail simulation impacts. Measurements of phase velocity for flexural wave propagation were made at four different frequencies (14, 25, 40, and 84 kHz) for both undamaged and damaged regions of the panels using a ZETEC Sondicator model S-9.

Phase velocity was measured in the undamaged regions using a probe with variable spacing (separation distance) between the transmitter and the receiver. An oscillating transverse load was applied through the transmitter, introducing flexural waves in the panel as illustrated below. The phase velocity was determined by monitoring the change in the received signal as the separation distance was increased.

In the damaged regions, phase velocity was measured using a probe with a fixed separation distance (0.75"). The probe was initially placed over an undamaged reference location where the phase velocity had already been measured. The probe was then moved in small increments to the center of the damaged region. The phase velocity was determined from the change in the received signal from the reference location to the measurement location.

Flexural Wave Damage Characterization

Input signal

Received signal reference location

Received signal measurement location

Amplitude

Time

Sender

Receiver

772
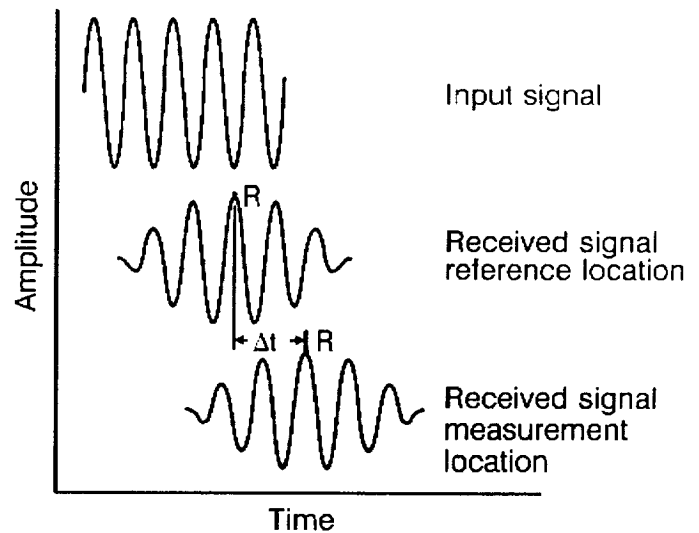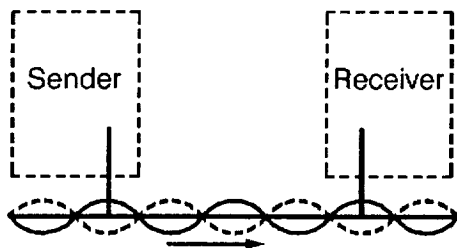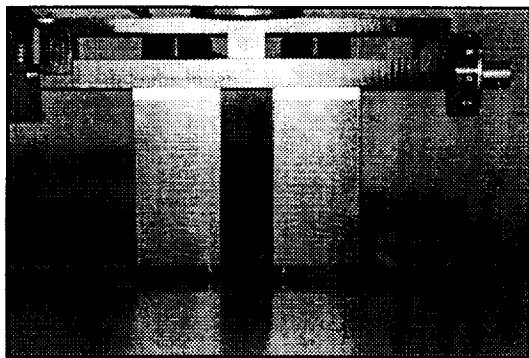
Phase velocities for the undamaged regions of the stiffened panels were predicted using the theoretical formulation of Tang, et al [13]. This formulation is based on laminated plate theory and includes the effects of transverse shear deformation and rotary inertia. The agreement between predicted and measured phase velocities was typically within 5% for the 32 panels studied. The comparison for one typical panel is shown in the figure.

The measured phase velocities in the damaged regions were lower than those in the undamaged regions. Since the measurements were made in the 0 degree direction, this decrease can be attributed to a reduction of the bending stiffness (D_{11}) and the transverse shear stiffness (A_{55}) in this direction [13]. In obtaining the estimates of stiffness reduction, D_{11} and A_{55} were assumed to be reduced by the same percentage. The theoretical model was used iteratively to determine what value of stiffness reduction gave the best fit to the data. An example is shown in the figure.

Stiffness Determination From Dispersion Curve

NASA/BOEING
ATCAS

ED-15
FL2014.15 s1h

773
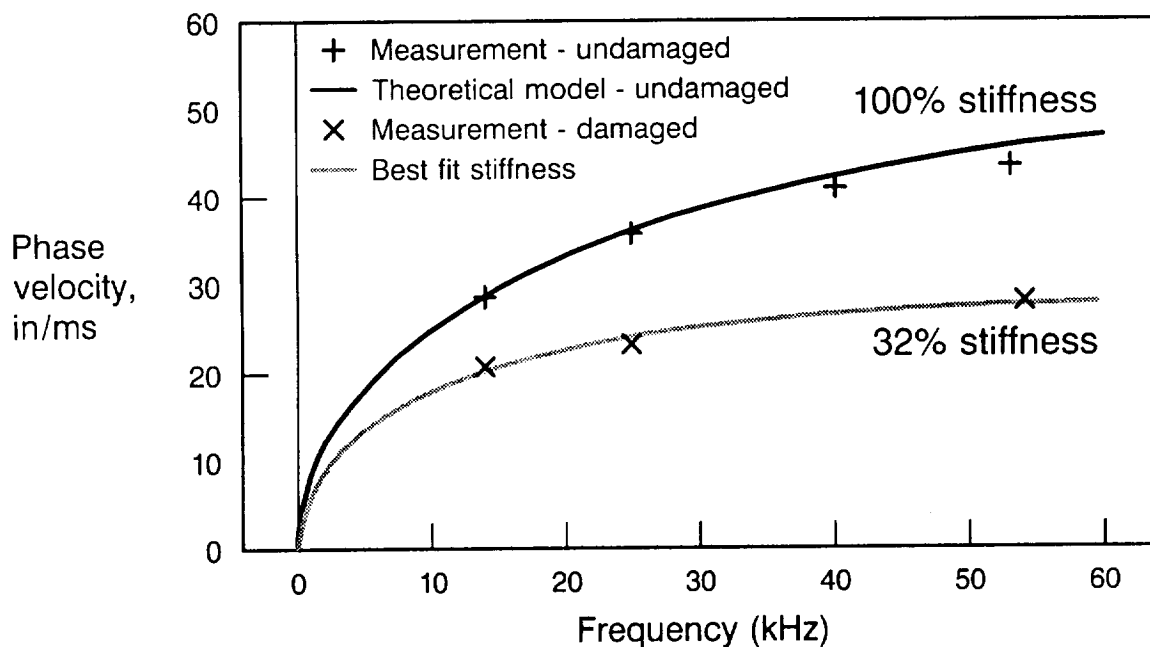
Mechanical bending tests were also performed on the panels for direct comparison to the stiffness estimates from the flexural wave inspections. Standard mechanical test machines could not be used because of the large size of the three-stringer panels (removal of the damaged regions from the panel was undesirable). Instead, a modified DYNATUP impactor at Integrated Technologies, Inc. was used to measure the load/deflection behavior.

The damaged region was centered over a ring shaped support (0.88" diameter) and a transverse load applied to the center of the region through a 0.25" diameter impact tup. Weights were then added to the cross-head and deflections measured using a dial indicator. The stiffness was taken to be the slope of the load versus deflection curve. Measurements were also made in an undamaged region of the panel to normalize the readings.

The large size of the panel in comparison to the test region created experimental difficulties. In particular, alignment of the panel was difficult and tipping of the panel was observed during some of the tests. The accuracy of these test results was estimated to be within 20 percent.
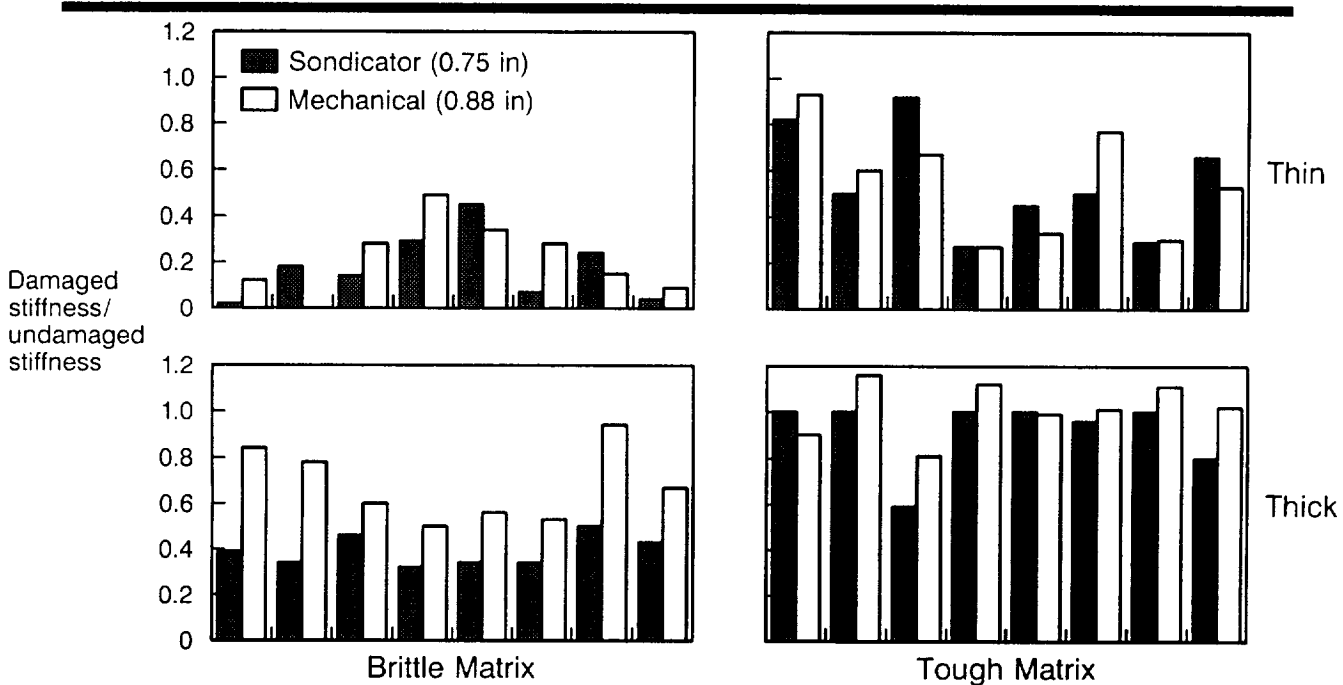
Mechanical Stiffness Tests
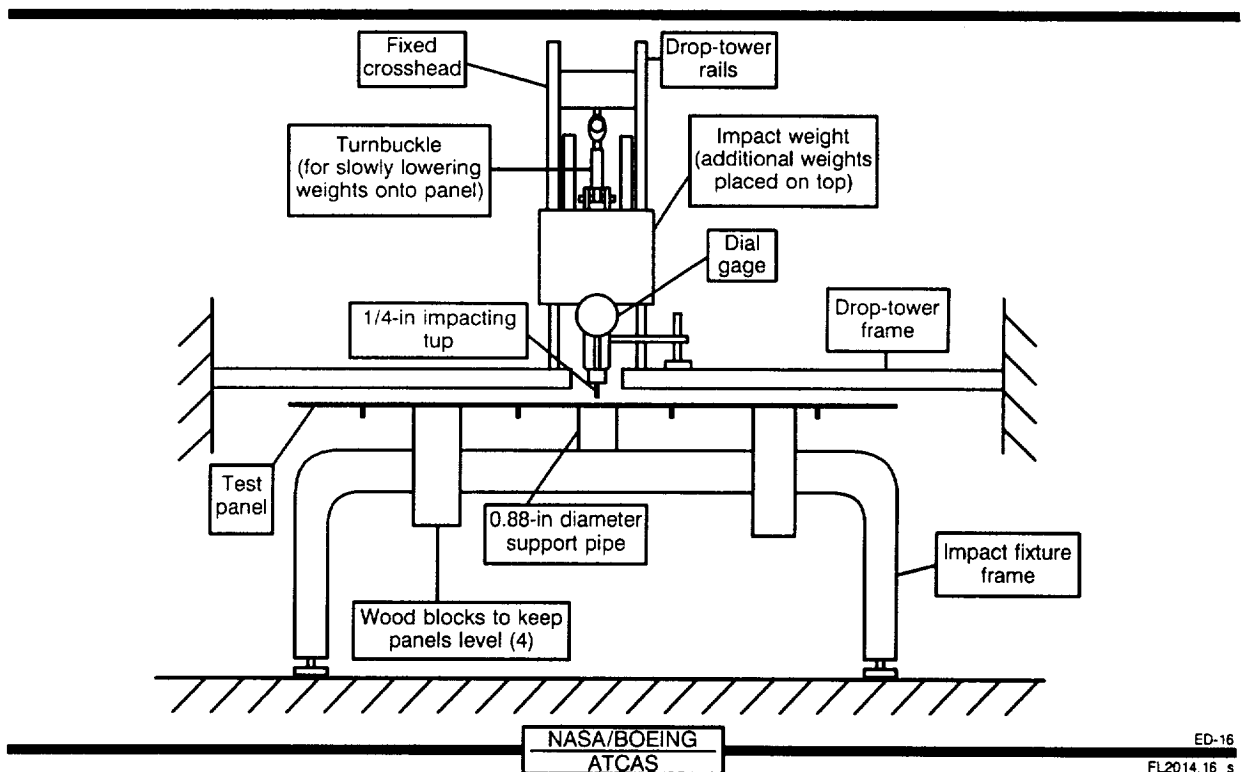
The normalized mechanically-measured stiffnesses are compared to the reduced stiffnesses measured using flexural wave propagation for all thirty-two hail simulation impacts. Note, each experimental run represents different combinations of the test variables (i.e., no replication of tests). The experimental runs were grouped by panel thickness and matrix toughness. The stiffness reduction resulting from the hail simulation impacts was strongly related to these two variables. The least stiffness reduction corresponded to the thicker panels with the tougher matrix materials. These results agree with the results of [3].

The stiffnesses measured in the flexural wave inspections agreed qualitatively with the those measured in the mechanical tests. However, the flexural wave inspections generally indicated a greater stiffness reduction than the mechanical tests. Some of this difference may have resulted from the inaccuracies in the mechanical tests. In addition, the flexural wave inspections were conducted in one direction only, whereas the mechanical measurements were related to the stiffnesses in multiple directions.

Comparison of Mechanical Tests and Sondicator Measurements

NASA/BOEING
ATCAS

ED-17
FL2014.17 s

The correlation between the mechanical measurements and the results of the flexural wave inspections was investigated. In addition, the mechanically measured stiffnesses were also compared to more traditional non-destructive measurements for assessing damage. The agreement was quantified using a Spearman rank correlation. The flexural wave inspection gave a better correlation to the mechanical stiffnesses than either the damage area measured by the C-scan or the indentation depth.

It should be noted that the mechanical measurements were made over a region smaller than the impact-damaged region for most panels. In order to fully characterize the damage, both the local stiffness reduction and the size of the damage area may be necessary. The size of the damaged region can be obtained through either flexural wave inspections or more traditional ultrasonic techniques.

Correlation With Mechanically Measured Stiffness

Mechanically Measured Stiffness (Damaged/Undamaged)
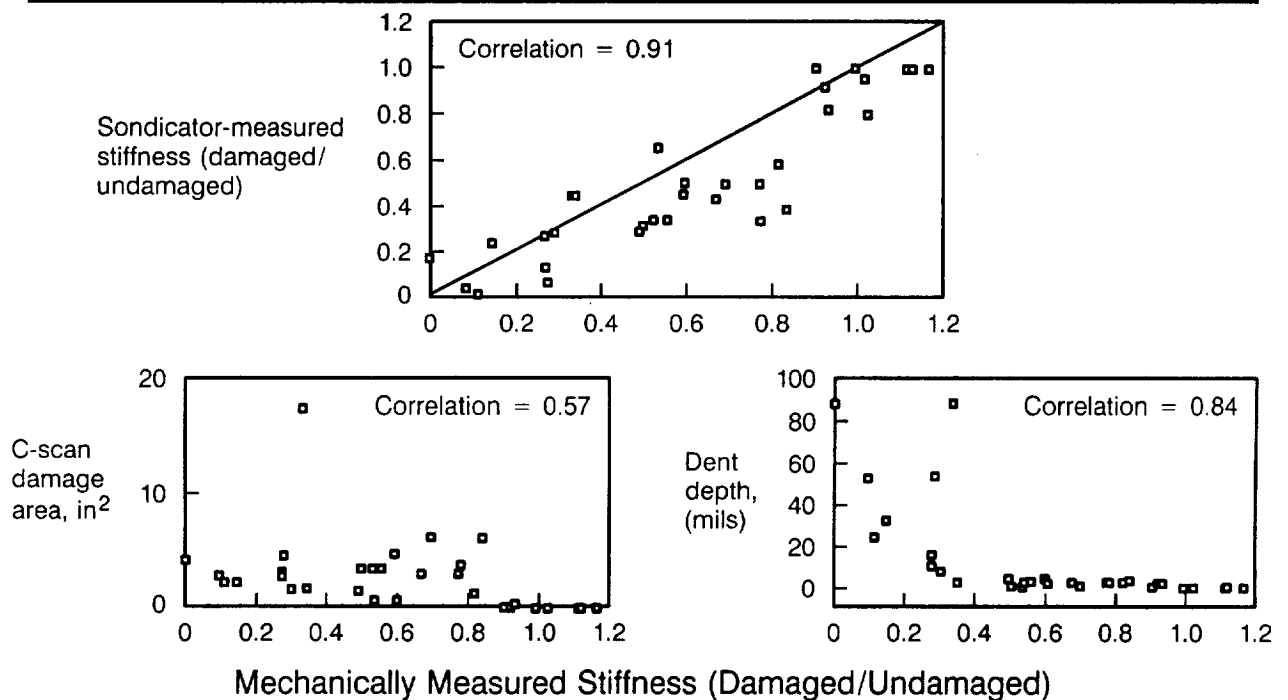
NASA/BOEING
ATCAS

ED-18
FL2014.18 s

C-4

Significant Effects

The reduced stiffnesses generated via the flexural wave measurements on the hail simulation impacts were analyzed using half-normal plots. Matrix type and laminate thickness were found to be statistically significant, as would be expected from observation of the previous figures. For comparison, important effects when examining the planar damage area response of the hail simulation impacts from Part 1 [3] were Matrix type and an interaction between Matrix type and Laminate thickness. Only three confounded two-way interactions are present because the extrinsic variables were eliminated from the hail simulation impacts. Fiber type may be considered significant if a more liberal interpretation of the half-normal plots is taken.

Local Flexural Stiffness

Significant Effects

Impact location	Variable	Low level	High level	Result
H	Laminate thickness, in	0.089	0.18	Increased
H	Matrix type	938	977-2	Increased
H	Fiber type*	AS4	IM7	Increased

Important Interactions

H Fiber type - Matrix or Fiber Volume - Material Form
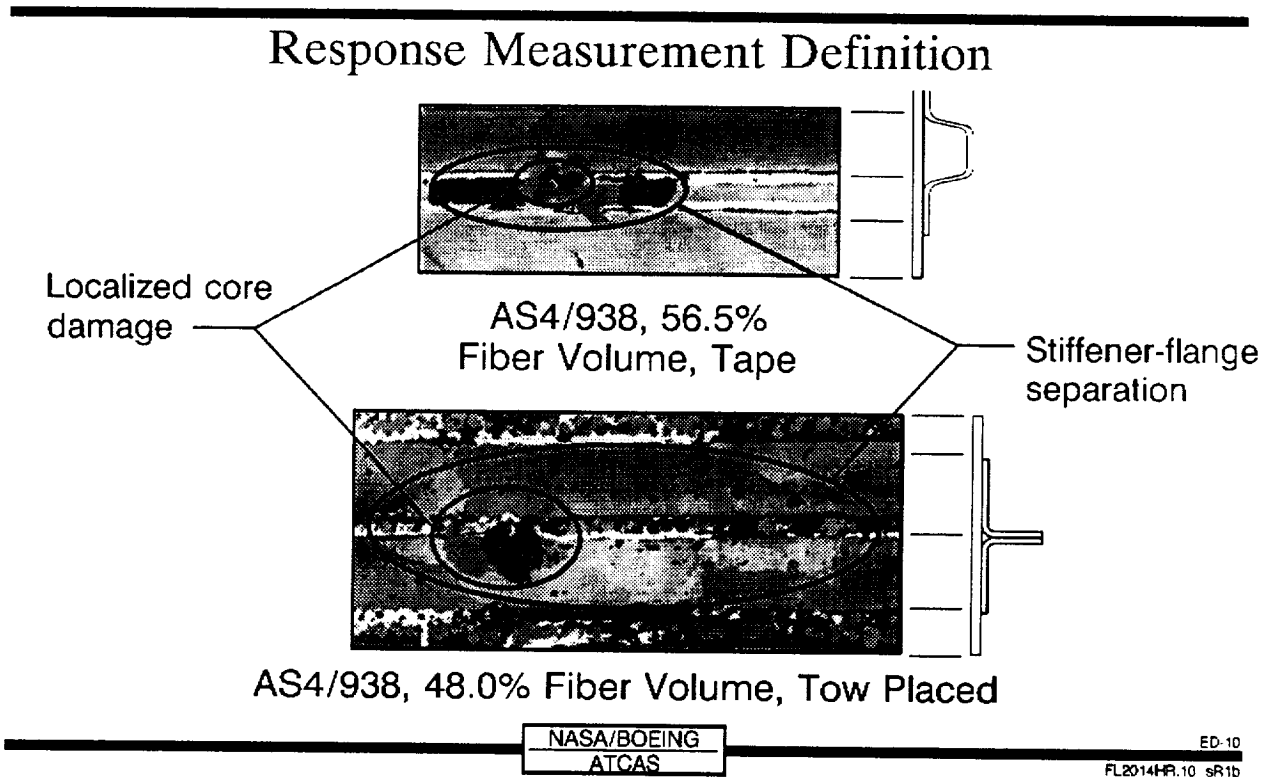
H ~~or Stiffener type - Stiffener spacing~~

H (Hail simulation)
* Potentially significant.

| NASA/BOEING |
| ATCAS |

ED-24
FL2014.24 hR3h

Response Measurement Definition

Matrix damage created in the stiffener flange edge and stiffener web impacts was studied using pulse-echo ultrasonics. These ultrasound results were presented as C-scans, with different colors representing a variation in depth of a reflective surface, such as a delamination or the back surface of the laminate. The matrix damage found in the stiffener impacts consisted of both a localized region of delaminations with interconnecting transverse cracks and a separation of the stiffener flange from the skin. The local region of damage is expected to effect the post-impact performance of the laminate through sublaminate stability and load redistribution similar to that observed in unstiffened laminate CAI tests. The stiffener flange separation region could act as an initial flaw in a stiffener separation event.

Matrix Damage

Response Measurement Definition

Localized core damage

AS4/938, 56.5% Fiber Volume, Tape

Stiffener-flange separation

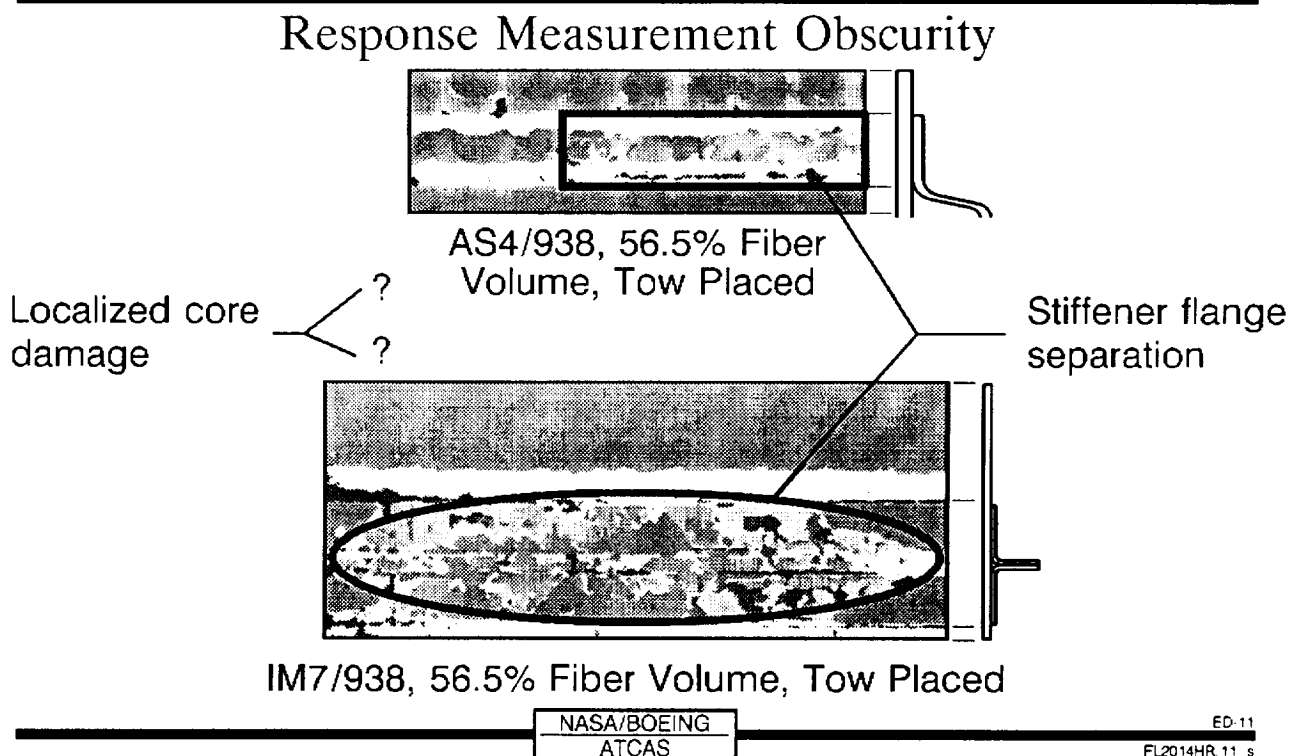AS4/938, 48.0% Fiber Volume, Tow Placed

Response Measurement Obscurity

Interpretation of the C-scan results was not always straightforward. The region associated with localized core damage was not always distinguishable from the stiffener separation area. Statistically, the missing data reduced the number of degrees of freedom in the results, lowering the resolution on certain variables.

The boundaries of the stiffener separation area were sometimes obscured by "noise" in the C-scans (e.g., signals caused by the tow placement microstructure). The subjective nature of some of the stiffener separation area measurements introduced uncertainty in the measurements. The variation created by this uncertainty adds to the overall experimental noise, which is accounted for by the statistical analysis.

Matrix Damage

Response Measurement Obscurity

AS4/938, 56.5% Fiber Volume, Tow Placed

Localized core damage ? ?

Stiffener flange separation

IM7/938, 56.5% Fiber Volume, Tow Placed

Significant Effects

The stiffener flange separation areas for both the flange edge and web impacts were analyzed using half-normal plots. The statistical analysis showed the variables listed below to significantly affect stiffener flange separation area created during the impact event. The letter preceding each variable indicates the data set (flange edge or web impact) for which the listed variable was found to be significant. A variable is significant for both sets of impacts if both letters are listed. In addition to the four main effects listed, four sets of two-way interactions are important. Each set of confounded two-way interactions listed include 4 others which were not listed for brevity.

Several observations can be made from these results. It is observed that matrix toughness influences the size of the separation area for the stiffener web impacts, although the influence is reduced when a layer of adhesive exists between the stiffener flange and the skin. The thicker panels tended to have more separation area than the thin panels for the stiffener flange edge impacts.

Stiffener-Flange Separation Area

Significant Effects

Impact location	Variable	Low level	High level	Result
F,W	Impact energy, in-lb	350	1600	Increased
W*	Matrix type	938	977-2	Decreased
F,W	Impactor diameter, in	0.25	1.00	Increased
F	Laminate thickness, in	0.089	0.18	Increased

Important Interactions

F,W	Material form - Skin layup (stiffener layup)	or	Matrix type - Stiffener type	or	?
F,W	Laminate thickness - Impactor energy	or	Fiber type - Fiber volume	or	?
W*	Matrix type - Impact energy	or	Material form - Laminate thickness (stiffener layup)	or	?
W*	Matrix type - Impactor diameter	or	Skin layup - Laminate thickness	or	?

*More important for no adhesive case   F (flange) W (web)

NASA/BOEING
ATCAS

ED-27
FL2014.27 HR2h

Significant Effects

The localized core damage area data sets for both the stiffener flange edge and stiffener web impacts were analyzed using half-normal plots. The statistical analysis showed the variables listed below to have significant effects on the localized core damage area created during the impact event. The letter preceding each variable indicates the data set for which the listed variable was found to be significant. A variable is significant for both sets of impacts if both letters are listed. In addition to the four main effects listed, three sets of two-way interactions are important. Each set of confounded two-way interactions listed includes four others which were not listed for brevity.

Several observations can be made from these results. It is observed that matrix toughness influences the localized core damage area for both the stiffener flange edge and stiffener web impacts. Stiffener type was statistically significant, with the hat stiffener having less localized core area. These results have been influenced by missing data points, resulting in lower resolution for the variables studied.

Localized Core-Damage Area

Significant Effects

Impact location	Variable	Low level	High level	Result
F,W	Impact energy, in-lb	350	1600	Increased
F,W	Impactor diameter, in	0.25	1.00	Increased
F,W	Matrix type	938	977-2	Decreased
F,W	Stiffener type	Blade	Hat	Decreased

Important Interactions

F Matrix type - Impactor diameter   or Skin layup - Laminate thickness or ?

F Impact energy - Impactor diameter   or Material form - Skin layup   or ?
                                             (stiffener layup)

W Material form - Impactor diameter   or Stiffener type - Impact energy   or ?

F (flange) W (web)

NASA/BOEING
ATCAS

ED-26
FL2014.26 hR3h

Response Measurement Definition

The influence of structural adhesive between the uncured skin and stiffener on stiffener separation area created during an impact event was examined. Two stiffener web impacts were performed on each panel, one on a stiffener with adhesive at the flange/skin interface and one on a stiffener without adhesive. The stiffener flange separation area for the stiffener without adhesive was divided by the separation area for the stiffener with adhesive. The larger the ratio the less influence the adhesive layer has on damage size. These results apply only to the stiffener separation area. The effect of an adhesive layer on other damage modes, such as fiber failure, has not been considered yet.

Stiffener Flange Separation Area - Adhesive/No Adhesive Ratio

Response Measurement Definition

782
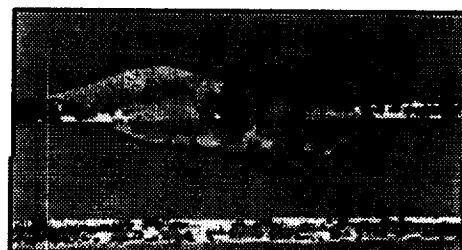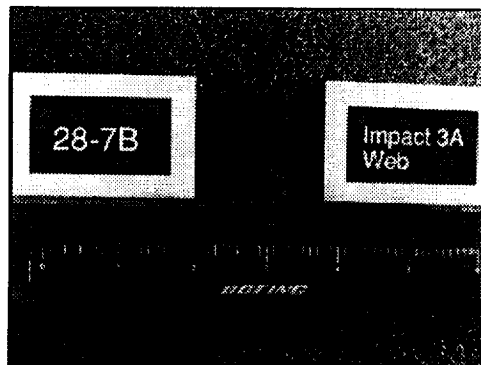
Significant Effects

Only three variables were found to be statistically significant for this data set. An increase in the ratio corresponds to the adhesive layer having less influence on the stiffener flange separation area. Based on these results, the addition of an adhesive layer is most beneficial for thin blade stiffened structure. The influence of the Skin layup variable could result from layers just outside of the flange to skin interface becoming critical locations for separation. The effect of Skin layup on stiffener separation should be further examined in future work.

Adhesive-to-No-Adhesive Ratio

Significant Effects

Impact location	Variable	Low level	High level	Result
W	Laminate thickness, in	0.089	0.18	Increased
W	Skin layup	Soft	Hard	Increased
W	Stiffener type	Blade	Hat	Increased

W (web)

The focus of the work accomplished in both Parts 1 and 2 of this study was to determine the statistically important variables and variable interactions for each measured response. Based on the results of this work, future impact damage studies for composite structure should consider, at a minimum, several levels of the extrinsic variables Impactor diameter and Impactor shape. A range of impact energies should also be included. The findings related to the intrinsic (structural design) variables have provided guidance to the NASA/Boeing ATCAS team on both material selection and structural test requirements and procedures. In addition, significant insight was gained into the impact phenomena and related criteria.

Summary

- Maximum force is strongly related to impactor mass.
- Flexural wave dispersion provides direct measure of local damage performance.
- Stiffener flange separation area is smaller when using a matrix with high interlaminar toughness.
- Stiffener-flange separation area increases with increasing thickness.
- Adhesive layer between skin and stiffener is most important for thin blade-stiffened structure.
- Impactor geometry and interactions between variables have strong influence on all measured responses.
- Teamwork is key to obtaining successful results.

NASA/BOEING	ED-31
ATCAS	FL2014.31 hR1s

This experiment has involved the efforts of a large number of people from various organizations within and outside of The Boeing Company. The authors wish to acknowledge all the personnel listed below for their technical support.

Contributors

Bill Avery - Boeing ATCAS Team

Roger Bennett - University of British Columbia

Todd Brown - Hercules Inc.

Greg Colvin - Zetec Inc.

Gordon Cox - Boeing Manufacturing R&D

Brian Coxon - Integrated Technology Inc.

Daniel Delfosse - University of British Columbia

Chris Eastland - Integrated Technology Inc.

Chuck Fitch - Zetec Inc.

Dodd Grande - Boeing Materials Technology

Carroll Grant - Hercules Inc.

Rich Groh - University of Washington

Ray Horton - Boeing ATCAS Team

Larry Ilcewicz - Boeing ATCAS Team

John Linn - Boeing Quality Assurance R&D

Bill Motzer - Boeing Quality Assurance R&D

Derek Newkirk - University of Washington

Linda Nuanez - Boeing Manufacturing R&D

G. Pageau - University of British Columbia

Anoush Poursartip - University of British Columbia

Ponce Puzon - Boeing Industrial Engineering

Peter Smith - Boeing ATCAS Team

Reza Vaziri - University of British Columbia

Kurt Willden - Boeing ATCAS Team

Rod Wishart - Integrated Technology Inc.

Mark Wood - Boeing Manufacturing R&D

NASA/BOEING
ATCAS

ED-25
FL2014.25 s

785

The results and observations presented to date have focused on individual responses only. Although this approach has provided significant insight into important aspects of impact damage resistance in composite fuselage structure, the results from the individual responses should be integrated to create a complete understanding. The relationships between criteria (visibility), applicable load levels (safe-flight, limit, or ultimate), and the types, magnitudes, and locations of the damage states must be understood in order to enhance the design optimization process.

Future Work

Integrate Understanding of Various Measured Responses
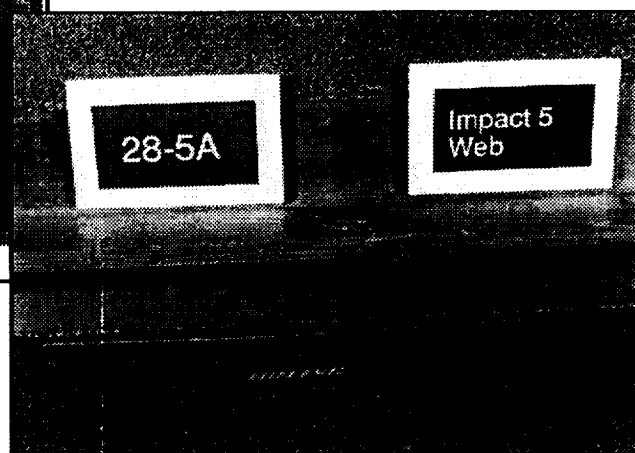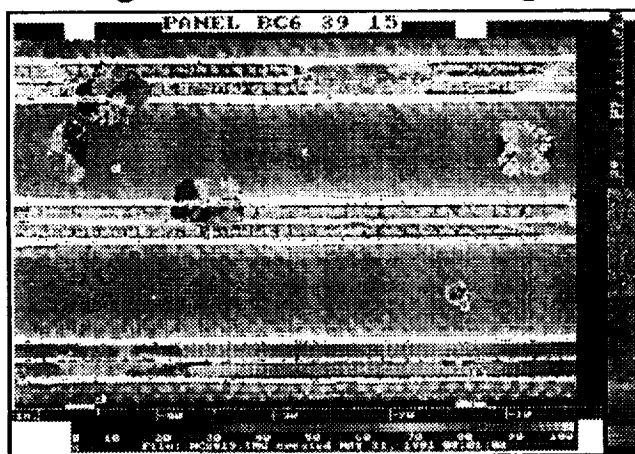
References

1. Dost, E. F., Ilcewicz, L. B., and Gosse, J. H., "Sublaminate Stability Based Modeling of Impact Damaged Composite Laminates," Proc. of 3rd Tech. Conf. of American Soc. for Composites, Technomic Publ. Co., 1988, pp. 354-363.

2. **Dost, E. F., Ilcewicz, L. B., and Avery, W. B., "The Effects of Stacking Sequence On Impact Damage Resistance and Residual Strength for Quasi-Isotropic Laminate," Composite Materials: Fatigue and Fracture, ASTM STP 1110, 1991.**

3. **Dost, E. F., Avery, W. B., Ilcewicz, L. B., Grande, D. H., and Coxon, B. R., "Impact Damage Resistance of Composite Fuselage Structure, Part I," Proc. of Ninth DoD/NASA/FAA Conf. on Fibrous Composites in Structural Design, FAA Publication, 1991.**

4. Wheeler, D. J., Understanding Industrial Experimentation, Statistical Process Controls, Inc., Knoxville, TN. 37919.

5. Milliken, G. A. and Johnson, D. E., Analysis of Messy Data. Volume1: Designed Experiments, Van Nostrand Reinhold Co., NY, 1984.

6. Milliken, G. A. and Johnson, D. E., Analysis of Messy Data. Volume2: Nonreplicated Experiments, Van Nostrand Reinhold Co., NY, 1989.

7. Winkel, J. D. and Adams, D. F., "Instrumented Drop Weight Impact Testing of Cross-Ply and Fabric Composites," Composites 16 No. 4, October 1985.

8. Whirley, R. G. and Hallquist, J. O., "DYNA3D - A Nonlinear, Explicit, Three-Dimensional Finite Element Code for Solid and Structural Mechanics - User Manual," University of California, Lawrence Livermore National Laboratory, Rept. UCRL-MA-107254, 1991.

9. **Ilcewicz, L. B., Dost, E. F., and Coggeshall, R. L., "A Model for Compression After Impact Strength Evaluation," Proc. of 21st International SAMPE Technical Conference, Soc. for Adv. of Material and Process Eng., 1989.**

10. **Dost, E. F., Finn, S. R., Stevens, J. J., Lin, K. Y., and Fitch, C. E., "Experimental Investigations into Composite Fuselage Impact Damage Resistance and Post-Impact Compression Behavior," Proc. of 37th International SAMPE Symposium & Exhibition, Soc. for Adv. of Material and Process Eng., 1992.**

11. Cairns, D. S. and Lagace P. A., "Residual Tensile Strength of Graphite/Epoxy and Kevlar/Epoxy Laminates with Impact Damage," Massachusetts Institute of Technology, TELAC Report 88-3, April, 1988.

12. Lamb, H., "On Waves in an Elastic Plate," Proc. of the Royal Society of London, Series A, 1917.

13. Tang, B., Henneke, E. G., and Stiffler, R. C., "Low Frequency Flexural Wave Propagation in Laminated Composite Plates," Proc. of Acousto-Ultrasonics: Theory and Application, 1988.

*References in bold were published while under Contract NAS1-18889.